A high physical accuracy method for incompressible magnetohydrodynamics

Michael A. Case* Alexander Labovsky †
Leo G. Rebholz‡ Nicholas E. Wilson§

Abstract

We present an energy, cross-helicity and magnetic helicity preserving method for solving incompressible magnetohydrodynamic equations with strong enforcement of solenoidal constraints. The method is a semi-implicit Galerkin finite element discretization, that enforces pointwise solenoidal constraints by employing the Scott-Vogelius finite elements. We prove the unconditional stability of the method and the optimal convergence rate. We also perform several numerical tests verifying the effectiveness of our scheme and, in particular, its clear advantage over using the Taylor-Hood finite elements.

1 Introduction

The conservation equations for incompressible magnetohydrodynamic (MHD) flows describe conducting, non-magnetic fluids, such as salt water, liquid metals, plasmas and strong electrolytes [7]. We will study finite element discretizations of the MHD equations in the following form, originally developed by Ladyzhenskaya, and studied in, e.g., [10, 18, 11, 12, 17]:

$$\begin{aligned} u_t + \nabla \cdot (uu^T) - Re^{-1}\Delta u + \frac{s}{2}\nabla(B\cdot B) - s\nabla \cdot BB^T + \nabla p &= f, && (1.1)\\ \nabla \cdot u &= 0, && (1.2)\\ B_t + Re_m^{-1}\nabla\times(\nabla\times B) + \nabla\times(B\times u) &= \nabla\times g, && (1.3)\\ \nabla\cdot B &= 0. && (1.4) \end{aligned}$$

Here, u is velocity, p is pressure, f is body force, $\nabla\times g$ is a forcing on the magnetic field B, Re is the Reynolds number, Re_m is the magnetic Reynolds number, and s is the coupling number.

We study a semi-implicit Galerkin finite element discretization of (1.1)-(1.4) which enforces pointwise solenoidal velocity and magnetic fields, as well as global conservation of

*Department of Mathematical Sciences, Clemson University, Clemson, SC 29634, mcase@clemson.edu. Partially supported by National Science Foundation grant DMS0914478.

†Department of Scientific Computing, Florida State University, Tallahassee FL 32306, alabovsky@fsu.edu. Partially supported by the US Air Force Office of Scientific Research under grant number FA9550-08-1-0415

‡Department of Mathematical Sciences, Clemson University, Clemson, SC 29634, rebholz@clemson.edu, http://www.math.clemson.edu/∼rebholz. Partially supported by National Science Foundation grant DMS0914478.

§Department of Mathematical Sciences, Clemson University, Clemson, SC 29634, newilso@clemson.edu. Partially supported by National Science Foundation grant DMS0914478.

energy and cross-helicity; by global conservation we mean the quantities are unchanged for ideal MHD with periodic boundary conditions, and in the viscous/resistance case and more general boundary conditions the quantities are exactly balanced, analogous to the continuous case. We also prove the exact conservation of magnetic helicity for the ideal MHD system, thus showing that our model preserves all three physical quantities that are conserved in the ideal MHD. In addition to proving these conservation laws, we also prove the scheme is unconditionally stable, well-posed, and optimally convergent. Lastly, several numerical experiments are given that demonstrate the effectiveness of the scheme.

Most schemes for fluid flow simulation conserve energy, but other fundamental conservation laws are often ignored or not strongly enforced. However, when these other laws are correctly accounted for in the numerical scheme, resulting solutions have greater *physical accuracy*, which leads to longer time stability and accuracy. For example, Arakawa's scheme for the 2D Navier-Stokes equations(NSE) that conserves energy and enstrophy[1], Arakawa and Lamb's scheme for the shallow water equations that conserves enstrophy and potential enstrophy [2] and those of Navon [19, 20], J.G. Liu and W. Wang's finite difference schemes for 3D axi-symmetric NSE flow that conserves energy and helicity [17] and MHD flows with symmetry that conserve energy and cross-helicity, and most recently a scheme for full 3D NSE that conserves energy and helicity [21, 6], all exhibit better long time behavior than comparable schemes that conserve only energy. The discretization we formulate and study herein for (1.1)-(1.4) is a finite element scheme that conserves all three fundamental quantities for general MHD flows - energy, cross-helicity and magnetic helicity, and is therefore also expected to exhibit good accuracy.

In addition to integral invariants, there are other conservation laws fundamental to the system (1.1)-(1.4), which are explicitly part of the continuous system as equations (1.2) and (1.4). Finite element discretizations typically enforce these laws weakly, however in MHD this is typically not sufficient. The problems that can arise from a poor enforcement of $\nabla \cdot u = 0$ are well known even for the simpler problems such as steady Navier-Stokes equations (NSE), see e.g. [15], and thus in the MHD system such physically inconsistent effects can be magnified. The requirement that $\nabla \cdot B = 0$ comes from the fact that B is derived as the curl of a electric field, and since $\operatorname{div}\operatorname{curl} = 0$ is a formal mathematical identity, for B not to be divergence free is mathematical inconsistency. This is well known in the MHD community, and algorithms that preserve incompressibility of B provided an incompressible initial condition is given exist [18], and for those that do not, techniques such as 'divergence cleansing' can be applied to recover mathematically plausible solutions [8]. The problem of satisfying the divergence-free condition for the magnetic field is crucial in many of the MHD applications; for instance, different numerical techniques have been used to prevent the incorrect shock capturing because of the violation of $\nabla \cdot B = 0$ condition. One can find the description of such techniques in [23] and references therein. Our scheme strongly enforces (pointwise!) the solenoidal constraints by coupling the discrete analog of (1.4) to (1.3) through the addition of a corresponding Lagrange multiplier λ to (1.3), then using the Scott-Vogelius element pair to approximate both (u, p) and (B, λ). Under mild restrictions, this element pair has recently been shown to be LBB stable and admits optimal approximation properties, and also implicitly enforces strong divergence free constraints when only weak enforcement is implemented [24]. It has since been successfully used with the steady and time-dependent NSE [4, 16, 15, 5], and thus the extension to using it for MHD is a next natural step.

There are two natural extensions of the scheme given in Section 3 for which our analysis is relevant. The first is for a linearization of the scheme via the method of Baker [3],

by linearly extrapolating the first term of the each of the four trilinear terms. All of the theory proven for the full nonlinear (Crank-Nicolson) scheme is still valid, although the convergence proof would have additional technical details. This scheme offers a significant increase in efficiency, since only one linear solve is needed at each timestep; all of our numerical experiments with the scheme will employ this linearization. The second extension is for Taylor-Hood elements, provided the trilinear terms are all skew-symmetrized. Here, the global conservation of energy and cross helicity still hold as does optimal convergence, however with this element choice, the incompressibility constraints are only weakly enforced. We show with a simple numerical example that, as expected, this element choice can give much worse results that Scott-Vogelius elements provide.

This report is arranged as follows. Section 2 presents notation and preliminaries, Section 3 derives the numerical scheme and proves conservation properties for it. Section 4 presents stability and convergence analysis for the scheme, and Section 5 discusses extensions of the scheme to a linearized form that still admits the conservation properties, and to the choice of Taylor-Hood elements. Section 6 gives several numerical experiments that show the effectiveness of the scheme.

2 Notation and Preliminaries

We consider a polygonal or polyhedral domain $\Omega \subset \mathbb{R}^d$ ($d = 2$ or 3), with Dirichlet boundary conditions for both velocity and the magnetic field. We denote the $L^2(\Omega)$ norm and inner product by $\|\cdot\|$ and $(\cdot,\cdot)$, respectively.

For simplicity, we consider the case of homogeneous Dirichlet conditions, but the extension to the general case can be made in the standard way [22]. Extension to periodic boundaries is trivial, but requires the domain be a box, and extension to most other boundary conditions is done in the usual way.

The Poincare-Freidrich's inequality will be used throughout our analysis: For $\phi \in H_0^1(\Omega)$,

$$\|\phi\| \leq C(\Omega) \|\nabla\phi\| .$$

The natural function spaces for our problem are

$$\begin{aligned} X = H_0^1(\Omega) &= \{v \in H^1(\Omega) \ : \ v = 0 \text{ on } \partial\Omega\} \\ Q = L_0^2(\Omega) &= \{q \in L^2(\Omega) \ : \ \int_\Omega q = 0\} \end{aligned}$$

The following lemma for bounding the trilinear forms will be used heavily in our analysis.

Lemma 2.1. *For $u, v, w \in X$, there exists $C = C(\Omega)$ such that*

$$(u \cdot \nabla v, w) \leq C \|\nabla u\| \|\nabla v\| \|v\|^{1/2} \|\nabla v\|^{1/2} \tag{2.1}$$

$$(u \cdot \nabla v, w) \leq C \|\nabla u\| \|\nabla v\| \|\nabla v\| \tag{2.2}$$

Proof. These estimates follow from Holder's inequality, the Sobolev imbedding theorem and Poincare-Freidrich's inequality. □

The finite element spaces used throughout will be the Scott-Vogelius pair, $(X_h, Q_h) = (P_k, P_{k-1}^{disc})$. We make the following two assumptions throughout this report:
A1: The mesh is created as a barycenter refinement of a regular mesh,
A2: The polynomial degree $k \geq d$.

Under these assumptions, this element pair is LBB stable and admits optimal approximation properties [24]. This pair will be used to approximate the velocity-pressure pair, and the magnetic field - Lagrange multiplier pair. A fundamentally important property of Scott-Vogelius elemetns is that the usual weak enforcement of incompressibility via

$$(\nabla \cdot v_h, q_h) = 0 \ \forall q_h \in Q_h,$$

implicitly enforces incompressibility pointwise since q_h can be chosen as $q_h = \nabla \cdot v_h$, which provides

$$\|\nabla \cdot v_h\|^2 = 0 \implies \nabla \cdot v_h = 0.$$

This property is important in the proposed numerical scheme for several reasons. First, mass conservation can be enforced pointwise via the usual weak enforcement of incompressibility of velocity. Second, the incompressibility of the magnetic field can be enforced pointwise in the same manner. Third, in all of our trilinear terms, skew-symmetry need not be enforced (for stability) as it would if, for example, Taylor-Hood elements were used; this provides a cheaper assembly time. Last, the use of Scott-Vogelius elements decouples the pressure error from the velocity error. The pressure in the numerical scheme we study is actually a modified pressure $P := p + \frac{s}{2}|B|^2$ (see below for more details), which can be significantly more complex than usual pressure. However, with Scott-Vogelius elements, larger pressure errors do not directly affect the velocity error as they do for most other common element choices [13, 14].

Define the space of discretely divergence free function as

$$V_h := \{v_h \in X_h \ : \ (\nabla \cdot v_h, q_h) = 0 \ \forall q_h \in Q_h\}.$$

Note that functions in V_h, when using the Scott-Vogelius pair, are pointwise divergence free.

3 Derivation of energy and helicities conserving scheme

There are three fundamental physical quantities conserved in the ideal MHD (in the absence of the forcing, with zero kinematic viscosity and magnetic diffusivity). These are the energy, cross-helicity and magnetic helicity, defined, respectively, as

$$\begin{aligned} E &= \frac{1}{2}\int_\Omega (u(x)\cdot u(x) + sB(x)\cdot B(x))dx, \\ H_C &= \frac{1}{2}\int_\Omega (u(x)\cdot B(x))dx, \\ H_M &= \frac{1}{2}\int_\Omega (\mathbb{A}(x)\cdot B(x))dx, \end{aligned}$$

where $\mathbb{A}$ is the vector potential, $B = \nabla \times \mathbb{A}$. We shall verify that all three of these quantities are conserved by our scheme.

We begin with the formulation (1.1)-(1.4), expand the curl operator in the (1.3) equation and use that $\nabla \cdot u = \nabla \cdot B = 0$ to get

$$u_t - Re^{-1}\Delta u + u\cdot\nabla u + \frac{s}{2}\nabla(B\cdot B) - sB\cdot\nabla B + \nabla p = f \quad (3.1)$$

$$\nabla \cdot u = 0 \quad (3.2)$$

$$B_t + Re_m^{-1}\nabla\times(\nabla\times B) + u\cdot\nabla B - B\cdot\nabla u = \nabla\times g \quad (3.3)$$

$$\nabla \cdot B = 0 \quad (3.4)$$

Denoting the modified pressure $P := p + \frac{s}{2}|B|^2$, using the vector identity

$$\Delta B = -\nabla \times (\nabla \times B) + \nabla(\nabla \times B),$$

and defining $\lambda := Re_m \nabla \cdot B (= 0)$ to act as a Lagrange multiplier corresponding to the solenoidal constraint of the magnetic field, we get

$$\begin{aligned} u_t - Re^{-1}\Delta u + u \cdot \nabla u - sB \cdot \nabla B + \nabla P &= f && (3.5)\\ \nabla \cdot u &= 0 && (3.6)\\ B_t - Re_m^{-1}\Delta B + u \cdot \nabla B - B \cdot \nabla u - \nabla \lambda &= \nabla \times g && (3.7)\\ \nabla \cdot B &= 0 && (3.8) \end{aligned}$$

The numerical scheme is now derived with a Galerkin finite element spatial discretization and (four leg) trapezoidal time discretization. Denote $u_h^{n+\frac{1}{2}} := \frac{1}{2}(u_h^n + u_h^{n+1})$. We require the discrete initial conditions to be pointwise divergence free, that is, u_h^0 and B_h^0 must be in V_h. Then $\forall (v_h, \chi_h, q_h, r_h) \in (X_h, X_h, Q_h, Q_h)$ find $(u_h^{n+1}, B_h^{n+1}, p_h^{n+\frac{1}{2}}, \lambda_h^{n+\frac{1}{2}}) \in (X_h, X_h, Q_h, Q_h)$ for $n = 0, 1, 2, ..., M = \frac{T}{\Delta t}$

$$\begin{aligned} &\frac{1}{\Delta t}(u_h^{n+1} - u_h^n, v_h) + (u_h^{n+\frac{1}{2}} \cdot \nabla u_h^{n+\frac{1}{2}}, v_h) + Re^{-1}(\nabla u_h^{n+\frac{1}{2}}, \nabla v_h)\\ &\quad -s(B_h^{n+\frac{1}{2}} \cdot \nabla B_h^{n+\frac{1}{2}}, v_h) - (P_h^{n+\frac{1}{2}}, \nabla \cdot v_h) = (f(t^{n+\frac{1}{2}}), v_h) && (3.9)\\ &\quad (\nabla \cdot u_h^{n+1}, q_h) = 0 && (3.10)\\ &\frac{1}{\Delta t}(B_h^{n+1} - B_h^n, \chi_h) + Re_m^{-1}(\nabla B_h^{n+\frac{1}{2}}, \nabla \chi_h) - (B_h^{n+\frac{1}{2}} \cdot \nabla u_h^{n+\frac{1}{2}}, \chi_h)\\ &\quad +(u_h^{n+\frac{1}{2}} \cdot \nabla B_h^{n+\frac{1}{2}}, \chi_h) + (\lambda_h^{n+\frac{1}{2}}, \nabla \cdot \chi_h) = (\nabla \times g(t^{n+\frac{1}{2}}), \chi_h) && (3.11)\\ &\quad (\nabla \cdot B_h^{n+1}, r_h) = 0 && (3.12) \end{aligned}$$

Lemma 3.1. *Solutions to the scheme* (3.9)-(3.12) *admit the following conservation laws:*

- *Mass conservation*

$$\nabla \cdot u_h^n = 0 \text{ (pointwise)} \tag{3.13}$$

- *Incompressibility of the magnetic field*

$$\nabla \cdot B_h^n = 0 \text{ (pointwise)} \tag{3.14}$$

- *Global energy conservation*

$$\begin{aligned} &\left(\left\|\frac{1}{2}u_h^M\right\|^2 + \frac{s}{2}\left\|B_h^M\right\|^2\right) + \Delta t \sum_{n=0}^{M-1}\left(Re^{-1}\left\|\nabla u_h^{n+\frac{1}{2}}\right\|^2 + sRe_m^{-1}\left\|\nabla B_h^{n+\frac{1}{2}}\right\|^2\right)\\ &= \left(\frac{1}{2}\left\|u_h^0\right\|^2 + \frac{s}{2}\left\|B_h^0\right\|^2\right) + \Delta t \sum_{n=0}^{M-1}\left((f(t^{n+\frac{1}{2}}), u_h^{n+\frac{1}{2}}) + s(\nabla \times g(t^{n+\frac{1}{2}}), B_h^{n+\frac{1}{2}})\right) \end{aligned} \tag{3.15}$$

- *Global cross-helicity conservation*

$$(u_h^M, B_h^M) + \Delta t \sum_{n=0}^{M-1} \left((Re^{-1} + Re_m^{-1})(\nabla u_h^{n+\frac{1}{2}}, \nabla B_h^{n+\frac{1}{2}}) \right)$$
$$= (u_h^0, B_h^0) + \Delta t \sum_{n=0}^{M-1} \left((\nabla \times g(t^{n+\frac{1}{2}}), u_h^{n+\frac{1}{2}}) + (f(t^{n+\frac{1}{2}}), B_h^{n+\frac{1}{2}}) \right) \quad (3.16)$$

Hence for $f = g = 0$ and $Re = Re_m = \infty$, we have exact conservation of both energy and cross-helicity.

- *Global magnetic helicity conservation in the case of ideal MHD*

$$(B_h^M, A_h^M) = (B_h^0, A_h^0), \text{ where } A \text{ is the vector potential, } B = \nabla \times A. \quad (3.17)$$

Proof. First, we note that for Scott-Vogelius elements, we can choose $q_h = \nabla \cdot u_h^{n+1}$ and $r_h = \nabla \cdot B_h^{n+1}$. Hence we have that $\nabla \cdot u_h^{n+1} = \nabla \cdot B_h^{n+1} = 0$, and thus that $\nabla \cdot u_h^{n+1/2} = \nabla \cdot B_h^{n+1/2} = 0$. This proves the first two conservation laws, and moreover these results will be used in the proofs of the other laws.

To prove energy conservation choose $v_h = u_h^{n+\frac{1}{2}}$ and $\chi_h = B_h^{n+\frac{1}{2}}$ which vanishes the second, fourth, and sixth terms in (3.9) and the fourth and fifth terms in (3.11), leaving

$$\frac{1}{2\Delta t}\left(\left\|u_h^{n+1}\right\|^2 - \|u_h^n\|^2 \right) + Re^{-1} \left\|\nabla u_h^{n+\frac{1}{2}}\right\|^2 - s(B_h^{n+\frac{1}{2}} \cdot \nabla B_h^{n+\frac{1}{2}}, u_h^{n+\frac{1}{2}})$$
$$= (f(t^{n+\frac{1}{2}}), u_h^{n+\frac{1}{2}}), \quad (3.18)$$
$$\frac{1}{2\Delta t}\left(\left\|B_h^{n+1}\right\|^2 - \|B_h^n\|^2 \right) + Re_m^{-1} \left\|\nabla B_h^{n+\frac{1}{2}}\right\|^2 - (B_h^{n+\frac{1}{2}} \cdot \nabla u_h^{n+\frac{1}{2}}, B_h^{n+\frac{1}{2}})$$
$$= (\nabla \times g(t^{n+\frac{1}{2}}), B_h^{n+\frac{1}{2}}). \quad (3.19)$$

Multiplying (3.19) by s, rewriting the nonlinear term in (3.18) as $-s(B_h^{n+\frac{1}{2}} \cdot \nabla B_h^{n+\frac{1}{2}}, u_h^{n+\frac{1}{2}}) = s(B_h^{n+\frac{1}{2}} \cdot \nabla u_h^{n+\frac{1}{2}}, B_h^{n+\frac{1}{2}})$, and adding (3.18) and (3.19) gives

$$\frac{1}{2\Delta t}(\left\|u_h^{n+1}\right\|^2 - \|u_h^n\|) + \frac{s}{2\Delta t}(\left\|B_h^{n+1}\right\|^2 - \|B_h^n\|^2) + Re^{-1} \left\|\nabla u_h^{n+\frac{1}{2}}\right\|^2$$
$$+ sRe_m^{-1} \left\|\nabla B_h^{n+\frac{1}{2}}\right\|^2 = (f(t^{n+\frac{1}{2}}), u_h^{n+\frac{1}{2}}) + s(\nabla \times g(t^{n+\frac{1}{2}}), B_h^{n+\frac{1}{2}}). \quad (3.20)$$

Multipling by Δt and summing over timesteps finishes the proof of (3.15).

To prove cross helicity is conserved we choose $v_h = B_h^{n+\frac{1}{2}}$ in (3.9) and $\chi_h = u_h^{n+\frac{1}{2}}$ in (3.11). This vanishes the fourth and fifth terms in (3.9) and third and fifth terms in (3.9), leaving

$$\frac{1}{\Delta t}(u_h^{n+1}-u_h^n,B_h^{n+\frac{1}{2}})+(u_h^{n+\frac{1}{2}}\cdot\nabla u_h^{n+\frac{1}{2}},B_h^{n+\frac{1}{2}})+Re^{-1}(\nabla u_h^{n+\frac{1}{2}},\nabla B_h^{n+\frac{1}{2}})$$
$$=(f(t^{n+\frac{1}{2}}),B_h^{n+\frac{1}{2}}), \tag{3.21}$$
$$\frac{1}{\Delta t}(B_h^{n+1}-B_h^n,u_h^{n+\frac{1}{2}})+Re_m^{-1}(\nabla B_h^{n+\frac{1}{2}},\nabla u_h^{n+\frac{1}{2}})+(u_h^{n+\frac{1}{2}}\cdot\nabla B_h^{n+\frac{1}{2}},u_h^{n+\frac{1}{2}})$$
$$=(\nabla\times g(t^{n+\frac{1}{2}}),u_h^{n+\frac{1}{2}}). \tag{3.22}$$

Adding (3.21) and (3.22) and noting that:

$$(u_h^{n+\frac{1}{2}}\cdot\nabla u_h^{n+\frac{1}{2}},B_h^{n+\frac{1}{2}})=-(u_h^{n+\frac{1}{2}}\cdot\nabla B_h^{n+\frac{1}{2}},u_h^{n+\frac{1}{2}}),\ \text{and} \tag{3.23}$$

$$\frac{1}{\Delta t}(u_h^{n+1}-u_h^n,B_h^{n+\frac{1}{2}})+\frac{1}{\Delta t}(B_h^{n+1}-B_h^n,u_h^{n+\frac{1}{2}}) \tag{3.24}$$
$$=\frac{1}{2\Delta t}\left((u_h^{n+1},B_h^{n+1})-(u_h^n,B_h^n)\right)+\frac{1}{2\Delta t}\left((u_h^{n+1},B_h^n)-(u_h^n,B_h^{n+1})\right) \tag{3.25}$$
$$+\frac{1}{2\Delta t}\left((B_h^{n+1},u_h^{n+1})-(B_h^n,u_h^n)\right)-\frac{1}{2\Delta t}\left((B_h^{n+1},u_h^n)-(B_h^n,u_h^{n+1})\right), \tag{3.26}$$

we get

$$\frac{1}{\Delta t}\left((u_h^{n+1},B_h^{n+1})-(u_h^n,B_h^n)\right)+(Re^{-1}+Re_m^{-1})(\nabla u_h^{n+\frac{1}{2}},\nabla B_h^{n+\frac{1}{2}})$$
$$=(\nabla\times g(t^{n+\frac{1}{2}}),u_h^{n+\frac{1}{2}})+(f(t^{n+\frac{1}{2}}),B_h^{n+\frac{1}{2}}) \tag{3.27}$$

Multiplying by Δt and summing over timesteps finishes the proof of (3.16).

Finally, choose $\chi_h=A_h^{n+\frac{1}{2}}$ in (3.11). In the absence of forcing and with zero magnetic diffusivity we obtain

$$\frac{1}{\Delta t}(B_h^{n+1}-B_h^n,A_h^{n+\frac{1}{2}})+(u_h^{n+\frac{1}{2}}\cdot\nabla B_h^{n+\frac{1}{2}},A_h^{n+\frac{1}{2}})-(B_h^{n+\frac{1}{2}}\cdot\nabla u_h^{n+\frac{1}{2}},A_h^{n+\frac{1}{2}})=0. \tag{3.28}$$

We will use the identity

$$((\nabla\times v)\times u,w)=(u\cdot\nabla v,w)-(w\cdot\nabla v,u). \tag{3.29}$$

Since the cross-product of two vectors is orthogonal to each of them,

$$((\nabla\times A_h^{n+\frac{1}{2}})\times u_h^{n+\frac{1}{2}},\nabla\times A_h^{n+\frac{1}{2}})=0. \tag{3.30}$$

It follows from (3.30) and (3.29) that

$$(u_h^{n+\frac{1}{2}}\cdot\nabla A_h^{n+\frac{1}{2}},\nabla\times A_h^{n+\frac{1}{2}})=((\nabla\times A_h^{n+\frac{1}{2}})\cdot\nabla A_h^{n+\frac{1}{2}},u_h^{n+\frac{1}{2}}). \tag{3.31}$$

Since $B_h^{n+\frac{1}{2}}=\nabla\times A_h^{n+\frac{1}{2}}$, we obtain

$$\frac{1}{2\Delta t}(B_h^{n+1}-B_h^n,A_h^{n+1}+A_h^n)=0,$$

and therefore

$$(\nabla\times A_h^{n+1},A_h^{n+1})=(\nabla\times A_h^n,A_h^n),$$

which completes the proof. □

4 Numerical analysis of the scheme

We prove in this section that the scheme is both unconditionally stable and optimally convergent.

Lemma 4.1. *Solutions to the scheme* (3.9)-(3.12) *are stable provided* $f \in L^2(0,T;H^{-1}(\Omega))$ *and* $g \in L^2(0,T;L^2(\Omega))$*, and satisfy*

$$\left(\left\|u_h^M\right\|^2 + s\left\|B_h^M\right\|^2\right) + \Delta t \sum_{n=0}^{M-1}\left(Re^{-1}\left\|\nabla u_h^{n+\frac{1}{2}}\right\|^2 + sRe_m^{-1}\left\|\nabla B_h^{n+\frac{1}{2}}\right\|^2\right)$$
$$\leq \left(\left\|u_h^0\right\|^2 + s\left\|B_h^0\right\|^2\right) + \Delta t \sum_{n=0}^{M-1}\left(Re\left\|f(t^{n+\frac{1}{2}})\right\|_{-1}^2 + sRe_m\left\|g(t^{n+\frac{1}{2}})\right\|^2\right) = C(Re, Re_m, f, g). \tag{4.1}$$

Proof. We begin this proof with the energy conservation equality (3.15),

$$\left(\left\|\frac{1}{2}u_h^M\right\|^2 + \frac{s}{2}\left\|B_h^M\right\|^2\right) + \Delta t \sum_{n=0}^{M-1}\left(Re^{-1}\left\|\nabla u_h^{n+\frac{1}{2}}\right\|^2 + sRe_m^{-1}\left\|\nabla B_h^{n+\frac{1}{2}}\right\|^2\right)$$
$$= \left(\frac{1}{2}\left\|u_h^0\right\|^2 + \frac{s}{2}\left\|B_h^0\right\|^2\right) + \Delta t \sum_{n=0}^{M-1}\left((f(t^{n+\frac{1}{2}}), u_h^{n+\frac{1}{2}}) + s(\nabla \times g(t^{n+\frac{1}{2}}), B_h^{n+\frac{1}{2}})\right) \tag{4.2}$$

The forcing term can be majorized with Cauchy-Schwarz and Young's inequalities to get

$$(f(t^{n+\frac{1}{2}}), u_h^{n+\frac{1}{2}}) \leq \frac{Re}{2}\left\|f(t^{n+\frac{1}{2}})\right\|_{-1}^2 + \frac{Re^{-1}}{2}\left\|\nabla u_h^{n+1/2}\right\|^2, \tag{4.3}$$

and similarly for the magnetic forcing term,

$$s(\nabla \times g(t^{n+\frac{1}{2}}), B_h^{n+\frac{1}{2}}) \leq \frac{sRe_m}{2}\left\|g(t^{n+\frac{1}{2}})\right\|^2 + \frac{sRe_m^{-1}}{2}\left\|\nabla B_h^{n+\frac{1}{2}}\right\|^2. \tag{4.4}$$

Using (4.3) and (4.4) in (4.2) gives

$$\left(\left\|u_h^M\right\|^2 + s\left\|B_h^M\right\|^2\right) + \Delta t \sum_{n=0}^{M-1}\left(Re^{-1}\left\|\nabla u_h^{n+\frac{1}{2}}\right\|^2 + sRe_m^{-1}\left\|\nabla B_h^{n+\frac{1}{2}}\right\|^2\right)$$
$$\leq \left(\left\|u_h^0\right\|^2 + s\left\|B_h^0\right\|^2\right) + \Delta t \sum_{n=0}^{M-1}\left(Re\left\|f(t^{n+\frac{1}{2}})\right\|_{-1}^2 + sRe_m\left\|g(t^{n+\frac{1}{2}})\right\|^2\right), \tag{4.5}$$

which proves the lemma. □

We now prove convergence of the scheme.

Theorem 4.1. *Assume* (u,p,B) *solves* (1.1)-(1.4) *and satisfying* $B_t, u_t \in L^2(\Omega,[0,T])$*,* $B_{tt}, u_{tt} \in L^2(\Omega,[0,T])$*,* $B_{ttt}, u_{ttt} \in L^2(\Omega,[0,T])$*, and* $B, u \in L^\infty(0,T;H^m(\Omega))$*, where* $m = \max(3,k)$*. Then the solution* $(u_h, p_h, B_h, \lambda_h)$ *to* (3.9)-(3.12) *converges to the true solution with optimal rate*

$$\|u - u_h\|_{2,1} + \|B - B_h\|_{2,1} = O(\Delta t^2 + h^k).$$

Proof. Multiply the momentum and magnetic equations (1.1), (1.3) at $t^{n+1/2}$ by $v_h \in V_h$ and $\chi_h \in V_h$, respectively, and integrate over the domain. Denoting $e_u^k = u_h^k - u^k$, $e_B^k = B_h^k - B^k$, we get

$$\begin{aligned}(u_t(t^{n+\frac{1}{2}}), v_h) + (u(t^{n+\frac{1}{2}}) \cdot \nabla u(t^{n+\frac{1}{2}}), v_h) + Re^{-1}(\nabla u(t^{n+\frac{1}{2}}), \nabla v_h) \\ - s(B(t^{n+\frac{1}{2}}) \cdot \nabla B(t^{n+\frac{1}{2}}), \nabla \cdot v_h) = (f(t^{n+\frac{1}{2}}), v_h))\end{aligned} \tag{4.6}$$

$$\begin{aligned}(B_t(t^{n+\frac{1}{2}}), \chi_h) + Re_m^{-1}(\nabla B(t^{n+\frac{1}{2}}), \nabla \chi_h) - (B(t^{n+\frac{1}{2}}) \cdot \nabla u(t^{n+\frac{1}{2}}), \chi_h) \\ + (u^{n+\frac{1}{2}} \cdot \nabla B^{n+\frac{1}{2}}, \chi_h) = (\nabla \times g(t^{n+\frac{1}{2}}), \chi_h).\end{aligned} \tag{4.7}$$

As usual, we will look to subtract the continuous formulation of the variational problem from the discrete formulation. We start this process by introducing the following terms (4.8)-(4.11), which replace the terms in the left-hand side of (4.6). To simplify notation, we use $\pm$ to denote adding and subtracting the same term.

$$\begin{aligned}(u_t(t^{n+\frac{1}{2}}), v_h) \pm \frac{1}{\Delta t}(u(t^{n+1}) - u(t^n), v_h) = \frac{1}{\Delta t}(u(t^{n+1}) - u(t^n), v_h) \\ + (u_t(t^{n+\frac{1}{2}}) - \{u(t^{n+1}) - u(t^n)\}\Delta t^{-1}, v_h).\end{aligned} \tag{4.8}$$

$$\begin{aligned}(u(t^{n+\frac{1}{2}}) \cdot \nabla u(t^{n+\frac{1}{2}}), v_h) \pm (u^{n+\frac{1}{2}} \cdot \nabla u^{n+\frac{1}{2}}, v_h) = (u(t^{n+\frac{1}{2}}) \cdot \nabla (u(t^{n+\frac{1}{2}}) - u^{n+\frac{1}{2}}), v_h) \\ + ((u(t^{n+\frac{1}{2}}) - u^{n+\frac{1}{2}}) \cdot \nabla u^{n+\frac{1}{2}}, v_h) + (u^{n+\frac{1}{2}} \cdot \nabla u^{n+\frac{1}{2}}, v_h).\end{aligned} \tag{4.9}$$

$$\begin{aligned}Re^{-1}\Big((\nabla u(t^{n+\frac{1}{2}}), \nabla v_h) \pm (\nabla u^{n+\frac{1}{2}}, \nabla v_h)\Big) \\ = Re^{-1}(\nabla (u(t^{n+\frac{1}{2}}) - u^{n+\frac{1}{2}}), \nabla v_h) + Re^{-1}(\nabla u^{n+\frac{1}{2}}, \nabla v_h)\end{aligned} \tag{4.10}$$

$$\begin{aligned}-s(B(t^{n+\frac{1}{2}}) \cdot \nabla B(t^{n+\frac{1}{2}}), v_h) \pm s(B^{n+\frac{1}{2}} \cdot \nabla B^{n+\frac{1}{2}}, v_h) = s(B^{n+\frac{1}{2}} \cdot \nabla (B^{n+\frac{1}{2}} - B(t^{n+\frac{1}{2}})), v_h) \\ + s((B^{n+\frac{1}{2}} - B(t^{n+\frac{1}{2}})) \cdot \nabla B(t^{n+\frac{1}{2}}), v_h) - s(B^{n+\frac{1}{2}} \cdot \nabla B^{n+\frac{1}{2}}, v_h).\end{aligned} \tag{4.11}$$

Now we can directly subtract (4.6) from (3.9),

$$\begin{aligned}\frac{1}{\Delta t}(e_u^{n+1} - e_u^n, v_h) + Re^{-1}(\nabla e_u^{n+\frac{1}{2}}, \nabla v_h) + (u_h^{n+\frac{1}{2}} \cdot \nabla e_u^{n+\frac{1}{2}}, v_h) + (e_u^{n+\frac{1}{2}} \cdot \nabla u^{n+\frac{1}{2}}, v_h) \\ - s(B_h^{n+\frac{1}{2}} \cdot e_B^{n+\frac{1}{2}}, v_h) - s(B_h^{n+\frac{1}{2}}] \cdot \nabla e_B^{n+\frac{1}{2}}, v_h) - s(e_B^{n+\frac{1}{2}} \cdot \nabla B^{n+\frac{1}{2}}, v_h) \\ = (u_t(t^{n+\frac{1}{2}}) - \{u(t^{n+1}) - u(t^n)\}\Delta t^{-1}, v_h) + Re^{-1}(\nabla (u(t^{n+\frac{1}{2}}) - u^{n+\frac{1}{2}}), \nabla v_h) \\ + (u(t^{n+\frac{1}{2}}) \cdot \nabla (u(t^{n+\frac{1}{2}}) - u^{n+\frac{1}{2}}), v_h) + ((u(t^{n+\frac{1}{2}}) - u^{n+\frac{1}{2}}) \cdot \nabla u^{n+\frac{1}{2}}, v_h) \\ + s((B^{n+\frac{1}{2}} - B(t^{n+\frac{1}{2}})) \cdot \nabla B(t^{n+\frac{1}{2}}), v_h) + s(B^{n+\frac{1}{2}} \cdot \nabla (B^{n+\frac{1}{2}} - B(t^{n+\frac{1}{2}})), v_h) =: G_1(t, B, u, v_h)\end{aligned} \tag{4.12}$$

Note that G_1 represents terms associated with interpolation error and are introduced to simplify the notation. Using the assumptions on the regularity of the solution, analysis similar to that in Chapter 3 will show

$$G_1(t, B, u, v_h) \leq C\Delta t^2 \|v_h\|. \tag{4.13}$$

Similar to the derivation of (4.12) we introduce terms (4.14)-(4.15) to the left hand side of (4.7) and then subtract from (3.11).

$$\begin{aligned}-(B(t^{n+\frac{1}{2}})\cdot\nabla u(t^{n+\frac{1}{2}}),\chi_h)\pm(B^{n+\frac{1}{2}}\cdot\nabla u^{n+\frac{1}{2}},\chi_h) &= (B(t^{n+\frac{1}{2}})\cdot\nabla(u^{n+\frac{1}{2}}-u(t^{n+\frac{1}{2}})),\chi_h)\\ &\quad+((B^{n+\frac{1}{2}}-B(t^{n+\frac{1}{2}}))\cdot\nabla u^{n+\frac{1}{2}},\chi_h)\\ &\quad-(B^{n+\frac{1}{2}}\cdot\nabla u^{n+\frac{1}{2}},\chi_h).\end{aligned} \tag{4.14}$$

$$\begin{aligned}&(u(t^{n+\frac{1}{2}})\cdot\nabla(B(t^{n+\frac{1}{2}})-B^{n+\frac{1}{2}}),\chi_h)\pm(u^{n+\frac{1}{2}}\cdot\nabla B^{n+\frac{1}{2}},\chi_h)\\ &\quad=(u(t^{n+\frac{1}{2}})\cdot\nabla(B(t^{n+\frac{1}{2}})-B^{n+\frac{1}{2}}),\chi_h)+((u(t^{n+\frac{1}{2}})-u^{n+\frac{1}{2}})\cdot\nabla B^{n+\frac{1}{2}},\chi_h)\\ &\qquad+(u^{n+\frac{1}{2}}\cdot\nabla B^{n+\frac{1}{2}},\chi_h)\end{aligned} \tag{4.15}$$

$$\begin{aligned}&\frac{1}{\Delta t}(e_B^{n+1}-e_B^n,\chi_h)+Re_m^{-1}(\nabla e_B^{n+\frac{1}{2}},\nabla\chi_h)-(B_h^{n+\frac{1}{2}}\cdot\nabla e_u^{n+\frac{1}{2}},\chi_h)\\ &\qquad-(e_B^{n+\frac{1}{2}}\cdot\nabla u^{n+\frac{1}{2}},\chi_h)+(u^{n+\frac{1}{2}}\cdot\nabla e_B^{n+\frac{1}{2}},\chi_h)+(e_u^{n+\frac{1}{2}}\cdot\nabla B^{n+\frac{1}{2}},\chi_h)\\ &\quad=(B_t(t^{n+\frac{1}{2}})-\{B(t^{n+1})-B(t^n)\}\Delta t^{-1},\chi_h)\\ &\qquad+Re_m^{-1}(\nabla(B(t^{n+\frac{1}{2}})-B^{n+\frac{1}{2}}),\nabla\chi_h)\\ &\qquad+(B(t^{n+\frac{1}{2}})\cdot\nabla(u^{n+\frac{1}{2}}-u(t^{n+\frac{1}{2}})),\chi_h)+((B^{n+\frac{1}{2}}-B(t^{n+\frac{1}{2}}))\cdot\nabla u^{n+\frac{1}{2}},\chi_h)\\ &\qquad+(u(t^{n+\frac{1}{2}})\cdot\nabla(B(t^{n+\frac{1}{2}})-B^{n+\frac{1}{2}}),\chi_h)+((u(t^{n+\frac{1}{2}})-u^{n+\frac{1}{2}})\cdot\nabla B^{n+\frac{1}{2}},\chi_h)\\ &\quad=G_2(t,B,u,\chi_h)\end{aligned} \tag{4.16}$$

Similar to G_1, we bound G_2 by

$$G_2(t,B,u,v_h)\le C\Delta t^2\|\chi_h\|. \tag{4.17}$$

Define $\phi_h^n=(u_h^n-U^n)$ and $\eta^n=(u^n-U^n)\Rightarrow e_u^n=\phi_h^n-\eta_u^n$ and analogously $e_B^n=(B_h^n-\mathcal{B}^n)+(\mathcal{B}^n-B^n)=\psi_h^n-\eta_B^n$. Where $U^k\in V_h$ and $\mathcal{B}^k\in V_h$. Substituting into (4.12) and (4.16) results in:

$$\begin{aligned}&\frac{1}{\Delta t}(\phi_h^{n+1}-\phi_h^n,v_h)+Re^{-1}(\nabla\phi_h^{n+\frac{1}{2}},\nabla v_h)+(u_h^{n+\frac{1}{2}}\cdot\nabla\phi_h^{n+\frac{1}{2}},v_h)+(\phi_h^{n+\frac{1}{2}}\cdot\nabla u^{n+\frac{1}{2}},v_h)\\ &\qquad-s(B_h^{n+\frac{1}{2}}\cdot\nabla\psi_h^{n+\frac{1}{2}},v_h)-s(\psi_h^{n+\frac{1}{2}}\cdot\nabla B^{n+\frac{1}{2}},v_h)\\ &\quad=\frac{1}{\Delta t}(\eta_u^{n+1}-\eta_u^n,v_h)+Re^{-1}(\nabla\eta_u^{n+\frac{1}{2}},\nabla v_h)+(u_h^{n+\frac{1}{2}}\cdot\nabla\eta_u^{n+\frac{1}{2}},v_h)\\ &\qquad+(\eta_u^{n+\frac{1}{2}}\cdot\nabla u^{n+\frac{1}{2}},v_h)-s(B_h^{n+\frac{1}{2}}\cdot\eta_B^{n+\frac{1}{2}},v_h)-s(B_h^{n+\frac{1}{2}}\cdot\nabla\eta_B^{n+\frac{1}{2}},v_h)\\ &\qquad-s(\eta_B^{n+\frac{1}{2}}\cdot\nabla B^{n+\frac{1}{2}},v_h)+G_1(t,u,B,v_h)\end{aligned} \tag{4.18}$$

$$\begin{aligned}\frac{1}{\Delta t}(\psi_h^{n+1}-\psi_h^n,\chi_h)+Re_m^{-1}(\nabla\psi_h^{n+1},\nabla\chi_h)-(B_h^{n+\frac{1}{2}}\cdot\nabla\phi_h^{n+\frac{1}{2}},\chi_h)-(\psi_h^{n+\frac{1}{2}}\cdot\nabla u^{n+\frac{1}{2}},\chi_h)\\ +(u^{n+\frac{1}{2}}\cdot\nabla\psi_h^{n+\frac{1}{2}},\chi_h)+(\phi_h^{n+\frac{1}{2}}\cdot\nabla B^{n+\frac{1}{2}},\chi_h)\\ =\frac{1}{\Delta t}(\eta_B^{n+1}-\eta_B^n,\chi_h)+Re_m^{-1}(\nabla\eta_B^{n+\frac{1}{2}},\nabla\chi_h)-(B_h^{n+\frac{1}{2}}\cdot\nabla\eta_u^{n+\frac{1}{2}},\chi_h)\\ -(\eta_B^{n+\frac{1}{2}}\cdot\nabla u^{n+\frac{1}{2}},\chi_h)+(u^{n+\frac{1}{2}}\cdot\nabla\eta_B^{n+\frac{1}{2}},\chi_h)+(\eta_u^{n+\frac{1}{2}}\cdot\nabla B^{n+\frac{1}{2}},\chi_h)\\ +G_2(t,u,B,\chi_h)\end{aligned}\tag{4.19}$$

Taking $\chi_h=\psi_h^{n+\frac{1}{2}}$ and $v_h=\phi_h^{n+\frac{1}{2}}$ into (4.18) and (4.19) and simplifying yields

$$\begin{aligned}\frac{1}{2\Delta t}(\|\phi_h^{n+1}\|^2-\|\phi_h^n\|^2)+Re^{-1}\left\|\nabla\phi_h^{n+\frac{1}{2}}\right\|^2+(\phi_h^{n+\frac{1}{2}}\cdot\nabla u^{n+\frac{1}{2}},\phi_h^{n+\frac{1}{2}})\\ -s(B_h^{n+\frac{1}{2}}\cdot\nabla\psi_h^{n+\frac{1}{2}},\phi_h^{n+\frac{1}{2}})-s(\psi_h^{n+\frac{1}{2}}\cdot\nabla B^{n+\frac{1}{2}},\phi_h^{n+\frac{1}{2}})\\ =\frac{1}{\Delta t}(\eta_u^{n+1}-\eta_u^n,\phi_h^{n+\frac{1}{2}})+Re^{-1}(\nabla\eta_u^{n+\frac{1}{2}},\nabla\phi_h^{n+\frac{1}{2}})+(u_h^{n+\frac{1}{2}}\cdot\nabla\eta_u^{n+\frac{1}{2}},\phi_h^{n+\frac{1}{2}})\\ +(\eta_u^{n+\frac{1}{2}}\cdot\nabla u^{n+\frac{1}{2}},\phi_h^{n+\frac{1}{2}})-s(B_h^{n+\frac{1}{2}}\cdot\nabla\eta_B^{n+\frac{1}{2}},\phi_h^{n+\frac{1}{2}})\\ -s(\eta_B^{n+\frac{1}{2}}\cdot\nabla B^{n+\frac{1}{2}},\phi_h^{n+\frac{1}{2}})+G_1(t,u,B,\phi_h^{n+\frac{1}{2}})\end{aligned}\tag{4.20}$$

$$\begin{aligned}\frac{1}{2\Delta t}(\left\|\psi_h^{n+\frac{1}{2}}\right\|^2-\left\|\psi_h^{n+\frac{1}{2}}\right\|^2)+Re_m^{-1}\left\|\nabla\psi_h^{n+\frac{1}{2}}\right\|^2-(B_h^{n+\frac{1}{2}}\cdot\nabla\phi_h^{n+\frac{1}{2}},\psi_h^{n+\frac{1}{2}})-(\psi_h^{n+\frac{1}{2}}\cdot\nabla u^{n+\frac{1}{2}},\psi_h^{n+\frac{1}{2}})\\ +(\phi_h^{n+\frac{1}{2}}\cdot\nabla B^{n+\frac{1}{2}},\psi_h^{n+\frac{1}{2}})=\frac{1}{\Delta t}(\eta_B^{n+1}-\eta_B^n,\psi_h^{n+\frac{1}{2}})+Re_m^{-1}(\nabla\eta_B^{n+\frac{1}{2}},\nabla\psi_h^{n+\frac{1}{2}})\\ -(B_h^{n+\frac{1}{2}}\cdot\nabla\eta_u^{n+\frac{1}{2}},\psi_h^{n+\frac{1}{2}})-(\eta_B^{n+\frac{1}{2}}\cdot\nabla u^{n+\frac{1}{2}},\psi_h^{n+\frac{1}{2}})+(u^{n+\frac{1}{2}}\cdot\nabla\eta_B^{n+\frac{1}{2}},\psi_h^{n+\frac{1}{2}})\\ +(\eta_u^{n+\frac{1}{2}}\cdot\nabla B^{n+\frac{1}{2}},\psi_h^{n+\frac{1}{2}})+G_2(t,u,B,\psi_h^{n+\frac{1}{2}})\end{aligned}\tag{4.21}$$

Using the inequality,

$$\frac{1}{\Delta t}(\eta^{n+1}-\eta_u^n,\phi_h^{n+\frac{1}{2}})\le\frac{1}{2\Delta t}\int_{t^n}^{t^{n+1}}\|\partial(\eta_u)\|^2\,dt+\frac{1}{2}\left\|\phi_h^{n+\frac{1}{2}}\right\|^2,\tag{4.22}$$

along with Hölder's Inequality and (4.13),

$$\frac{1}{2\Delta t}(\left\|\phi_h^{n+1}\right\|^2 - \|\phi_h^n\|^2) + \frac{Re^{-1}}{2}\left\|\nabla\phi_h^{n+\frac{1}{2}}\right\|^2 \leq \frac{1}{2\Delta t}\int_{t^n}^{t^{n+1}} \|\partial_t(\eta_u)\|^2\, dt + \frac{1}{2}\left\|\phi_h^{n+\frac{1}{2}}\right\|^2 + \left(\frac{Re^{-1}}{2}\right)\left\|\eta_u^{n+\frac{1}{2}}\right\|^2 + \left\|\nabla u^{n+\frac{1}{2}}\right\|_\infty \left\|\phi_h^{n+\frac{1}{2}}\right\|^2 + s(B_h^{n+\frac{1}{2}}\cdot\nabla\psi_h^{n+\frac{1}{2}}, \phi_h^{n+\frac{1}{2}}) + s\left\|\nabla B^{n+\frac{1}{2}}\right\|_\infty \left\|\psi_h^{n+\frac{1}{2}}\right\|\left\|\phi_h^{n+\frac{1}{2}}\right\| + C\left\|\nabla u_h^{n+\frac{1}{2}}\right\|\left\|\nabla\eta_u^{n+\frac{1}{2}}\right\|\left\|\nabla\phi_h^{n+\frac{1}{2}}\right\| + \left\|\nabla u^{n+\frac{1}{2}}\right\|_\infty \left\|\eta_u^{n+\frac{1}{2}}\right\|\left\|\phi_h^{n+\frac{1}{2}}\right\| + Cs\left\|\nabla B_h^{n+\frac{1}{2}}\right\|\left\|\nabla\eta_B^{n+\frac{1}{2}}\right\|\left\|\nabla\phi_h^{n+\frac{1}{2}}\right\| + s\left\|\nabla B^{n+\frac{1}{2}}\right\|_\infty \left\|\eta_B^{n+\frac{1}{2}}\right\|\left\|\phi_h^{n+\frac{1}{2}}\right\| + C\Delta t^2\left\|\phi_h^{n+\frac{1}{2}}\right\| \quad (4.23)$$

This reduces, with Cauchy-Schwarz and Young's inequalities and the assumption of the regularity of the solution, to

$$\frac{1}{2\Delta t}(\left\|\phi_h^{n+1}\right\|^2 - \|\phi_h^n\|^2) + \frac{Re^{-1}}{4}\left\|\nabla\phi_h^{n+\frac{1}{2}}\right\|^2 \leq \frac{1}{2\Delta t}\int_{t^n}^{t^{n+1}} \|\partial_t(\eta_u)\|^2\, dt + \left(\frac{Re^{-1}}{2}\right)\left\|\eta_u^{n+\frac{1}{2}}\right\|^2 + C(\left\|\phi_h^{n+\frac{1}{2}}\right\|^2 + \left\|\psi_h^{n+\frac{1}{2}}\right\|^2 + \Delta t^4 + \left\|\eta_u^{n+\frac{1}{2}}\right\|^2 + \left\|\nabla u_h^{n+\frac{1}{2}}\right\|^2\left\|\nabla\eta_u^{n+\frac{1}{2}}\right\|^2 + s^2\left\|\nabla B_h^{n+\frac{1}{2}}\right\|^2\left\|\nabla\eta_B^{n+\frac{1}{2}}\right\|^2 + s^2\left\|\eta_B^{n+\frac{1}{2}}\right\|^2) + s(B_h^{n+\frac{1}{2}}\cdot\nabla\psi_h^{n+\frac{1}{2}}, \phi_h^{n+\frac{1}{2}}) \quad (4.24)$$

We now step back from (4.24) and return to (4.21), which implies

$$\frac{1}{2\Delta t}(\left\|\psi_h^{n+1}\right\|^2 - \|\psi_h^n\|^2) + \frac{Re_m^{-1}}{2}\left\|\nabla\psi_h^{n+1/2}\right\|^2 \leq \frac{1}{2\Delta t}\int_{t^n}^{t^{n+1}} \|\partial_t(\eta_B)\|^2\, dt + \frac{1}{2}\left\|\psi_h^{n+\frac{1}{2}}\right\|^2 + Re_m^{-1}\left\|\nabla\eta_B^{n+\frac{1}{2}}\right\|^2 + (B_h^{n+\frac{1}{2}}\cdot\nabla\phi_h^{n+\frac{1}{2}}, \psi_h^{n+\frac{1}{2}}) + \left\|\nabla B^{n+\frac{1}{2}}\right\|_\infty \left\|\phi_h^{n+\frac{1}{2}}\right\|\left\|\psi_h^{n+\frac{1}{2}}\right\| + \left\|\nabla u^{n+\frac{1}{2}}\right\|_\infty \left\|\psi_h^{n+\frac{1}{2}}\right\|^2 + C\left\|\nabla B_h^{n+\frac{1}{2}}\right\|\left\|\nabla\eta_u^{n+\frac{1}{2}}\right\|\left\|\nabla\psi_h^{n+\frac{1}{2}}\right\| + C\left\|\nabla u^{n+\frac{1}{2}}\right\|_\infty \left\|\nabla\eta_B^{n+\frac{1}{2}}\right\|\left\|\psi_h^{n+\frac{1}{2}}\right\| + \left\|\nabla B^{n+\frac{1}{2}}\right\|_\infty \left\|\eta_u^{n+\frac{1}{2}}\right\|\left\|\psi_h^{n+\frac{1}{2}}\right\| + C\Delta t^2\left\|\psi_h^{n+\frac{1}{2}}\right\|. \quad (4.25)$$

Under the regularity assumptions, Cauchy-Schwarz and Young's inequalities, this can be reduced to

$$\frac{1}{2\Delta t}(\left\|\psi_h^{n+1}\right\|^2 - \|\psi_h^n\|^2) + \frac{Re_m^{-1}}{4}\left\|\nabla\psi_h^{n+1}\right\|^2 \leq \frac{1}{2\Delta t}\int_{t^n}^{t^{n+1}} \|\partial_t(\eta_B)\|^2\, dt + Re_m^{-1}\left\|\nabla\eta_B^{n+\frac{1}{2}}\right\|^2 + C(\left\|\psi_h^{n+\frac{1}{2}}\right\|^2 + \Delta t^4 + \left\|\phi_h^{n+\frac{1}{2}}\right\|^2 + \left\|\nabla\eta_B^{n+\frac{1}{2}}\right\|^2 + \left\|\eta_u^{n+\frac{1}{2}}\right\|^2 + Re\left\|\nabla B_h^{n+\frac{1}{2}}\right\|^2\left\|\nabla\eta_u^{n+\frac{1}{2}}\right\|^2) + (B_h^{n+\frac{1}{2}}\cdot\nabla\phi_h^{n+\frac{1}{2}}, \psi_h^{n+\frac{1}{2}}). \quad (4.26)$$

Multiplying (4.26) by s and adding it to (4.24), and using that

$$(B_h^{n+\frac{1}{2}}\cdot\nabla\phi_h^{n+\frac{1}{2}}, \psi_h^{n+\frac{1}{2}}) = -(B_h^{n+\frac{1}{2}}\cdot\nabla\psi_h^{n+\frac{1}{2}}, \phi_h^{n+\frac{1}{2}}),$$

along with the Poincare inequality and reducing, we get

$$\frac{1}{2\Delta t}(\left\|\phi_h^{n+1}\right\|^2-\|\phi_h^n\|^2)+\frac{s}{2\Delta t}(\left\|\psi_h^{n+1}\right\|^2-\|\psi_h^n\|^2)+\frac{Re^{-1}}{4}\left\|\nabla\phi_h^{n+\frac{1}{2}}\right\|^2+\frac{sRe_m^{-1}}{4}\left\|\nabla\psi_h^{n+1/2}\right\|^2$$
$$\leq\frac{1}{2\Delta t}\int_{t^n}^{t^{n+1}}\|\partial_t(\eta_u)\|^2\,dt+\frac{s}{2\Delta t}\int_{t^n}^{t^{n+1}}\|\partial_t(\eta_B)\|^2\,dt+\left(\frac{Re^{-1}}{2}\right)\left\|\eta_u^{n+\frac{1}{2}}\right\|^2+sRe_m^{-1}\left\|\nabla\eta_B^{n+\frac{1}{2}}\right\|^2$$
$$+C(s)(\left\|\phi_h^{n+\frac{1}{2}}\right\|^2+\left\|\psi_h^{n+\frac{1}{2}}\right\|^2+\Delta t^4+\left\|\eta_u^{n+\frac{1}{2}}\right\|^2+\left\|\nabla u_h^{n+\frac{1}{2}}\right\|^2\left\|\nabla\eta_u^{n+\frac{1}{2}}\right\|^2+\left\|\nabla B_h^{n+\frac{1}{2}}\right\|^2\left\|\nabla\eta_B^{n+\frac{1}{2}}\right\|^2$$
$$+\left\|\nabla\eta_B^{n+\frac{1}{2}}\right\|^2+Re\left\|\nabla B_h^{n+\frac{1}{2}}\right\|^2\left\|\nabla\eta_u^{n+\frac{1}{2}}\right\|^2) \quad (4.27)$$

Multiplying by $2\Delta t$ and summing over timesteps now gives

$$\left\|\phi_h^M\right\|^2+s\left\|\psi_h^M\right\|^2+\sum_{n=0}^{M-1}\left(Re^{-1}\left\|\nabla\phi_h^{n+\frac{1}{2}}\right\|^2+sRe_m^{-1}\left\|\nabla\psi_h^{n+\frac{1}{2}}\right\|^2\right)$$
$$\leq\int_0^T\left(\|\partial_t(\eta_u)\|^2+s\|\partial_t(\eta_B)\|^2\right)dt+CT\Delta t^4+C\Delta t\sum_{n=0}^{M-1}(\left\|\nabla\eta_u^{n+\frac{1}{2}}\right\|^2+\left\|\nabla\eta_B^{n+\frac{1}{2}}\right\|^2$$
$$+\left\|\nabla u_h^{n+\frac{1}{2}}\right\|^2\left\|\nabla\eta_u^{n+\frac{1}{2}}\right\|^2+\left\|\nabla B_h^{n+\frac{1}{2}}\right\|^2\left\|\nabla\eta_B^{n+\frac{1}{2}}\right\|^2+\left\|\nabla B_h^{n+\frac{1}{2}}\right\|^2\left\|\nabla\eta_u^{n+\frac{1}{2}}\right\|^2)$$
$$+C\sum_{n=1}^{M}(\left\|\phi_h^{n+1}\right\|^2+\left\|\psi_h^{n+1}\right\|^2) \quad (4.28)$$

Next we use approximation properties of the spaces and the stability estimate, which reduces (4.28) to

$$\left\|\phi_h^M\right\|^2+s\left\|\psi_h^M\right\|^2+\sum_{n=0}^{M-1}\left(Re^{-1}\left\|\nabla\phi_h^{n+\frac{1}{2}}\right\|^2+sRe_m^{-1}\left\|\nabla\psi_h^{n+\frac{1}{2}}\right\|^2\right)$$
$$\leq C(\Delta t^4+h^{2k})+C\sum_{n=1}^{M}(\left\|\phi_h^{n+1}\right\|^2+\left\|\psi_h^{n+1}\right\|^2) \quad (4.29)$$

Applying the Gronwall inequality followed by the triangle inequality completes the proof. □

5 Variations of the scheme

There are variations of this scheme for which most or all of the proven theoretical results still hold.

5.1 A linearization that maintains both physical and asymptotic accuracy

For many evolution equations, certain circumstances can allow linearizations can often be solved instead of the full nonlinear system, provided the particular linearization maintains stability and asymptotic accuracy. For the system (3.9)-(3.12) proposed herein, we found a linearization that preserves all of the conservation properties proved above, as well as

unconditional stability and optimal accuracy. The linearization is in the spirit of Baker's NSE linearization [3], where the first term of the nonlinearity is a second order in time extrapolation of known values. For the system (3.9)-(3.12), there are multiple nonlinear terms, and if the first term in each uses the extrapolation of Baker, then all of the proofs above will follow identically, except for convergence which will require slightly more work due to the new terms. Denoting the known functions

$$\begin{aligned}\widetilde{U}_h^n &:= \frac{3}{2}u_h^n - \frac{1}{2}u_h^{n-1},\\ \widetilde{B}_h^n &:= \frac{3}{2}B_h^n - \frac{1}{2}B_h^{n-1},\end{aligned}$$

the linearized scheme at each time step is given by, $\forall (v_h, \chi_h, q_h, r_h) \in (X_h, X_h, Q_h, Q_h)$,

$$\begin{aligned}&\frac{1}{\Delta t}(u_h^{n+1} - u_h^n, v_h) + (\widetilde{U}_h^n \cdot \nabla u_h^{n+\frac{1}{2}}, v_h) + Re^{-1}(\nabla u_h^{n+\frac{1}{2}}, \nabla v_h)\\ &+\frac{s}{2}(\widetilde{B}_h^n \cdot B_h^{n+\frac{1}{2}}, \nabla \cdot v_h) - s(\widetilde{B}_h^n \cdot \nabla B_h^{n+\frac{1}{2}}, v_h) - (p_h^{n+\frac{1}{2}}, \nabla \cdot v_h) = (f(t^{n+\frac{1}{2}}), v_h) \qquad (5.1)\\ &(\nabla \cdot u_h^{n+1}, q_h) = 0 \qquad (5.2)\\ &\frac{1}{\Delta t}(B_h^{n+1} - B_h^n, \chi_h) + Re_m^{-1}(\nabla B_h^{n+\frac{1}{2}}, \nabla \chi_h) - (\widetilde{B}_h^n \cdot \nabla u_h^{n+\frac{1}{2}}, \chi_h)\\ &+(\widetilde{U}_h^n \cdot \nabla B_h^{n+\frac{1}{2}}, \chi_h) + (\lambda_h^{n+\frac{1}{2}}, \nabla \cdot \chi_h) = (\nabla \times g(t^{n+\frac{1}{2}}), \chi_h) \qquad (5.3)\\ &(\nabla \cdot B_h^{n+1}, r_h) = 0 \qquad (5.4)\end{aligned}$$

Since this is a 2 step method, defining $u_h^{-1} := u_h^0$ and $B_h^{-1} := B_h^0$ is sufficient to maintain all the theoretical results.

5.2 Computing the scheme with Taylor-Hood elements

With Taylor-Hood elements, an important difference is that the velocity and magnetic field approximations will no longer be pointwise divergence free. Hence it will be necessary for stability to skew-symmetrize the nonlinear terms, and to combine the pressure in the momentum equation with the gradient term resulting from the nonlinear coupling of the magnetic field term. If we define the skew-symmetric operator

$$b^*(u, v, w) := \frac{1}{2}(u \cdot \nabla v, w) - \frac{1}{2}(u \cdot \nabla w, v),$$

and let P_h be a modified pressure term, we get the linear scheme, $\forall (v_h, \chi_h, q_h, r_h) \in (X_h, X_h, Q_h, Q_h)$,

$$\begin{aligned}&\frac{1}{\Delta t}(u_h^{n+1} - u_h^n, v_h) + b^*(\widetilde{U}_h^n, u_h^{n+\frac{1}{2}}, v_h) + Re^{-1}(\nabla u_h^{n+\frac{1}{2}}, \nabla v_h)\\ &-sb^*(\widetilde{B}_h^n, B_h^{n+\frac{1}{2}}, v_h) - (P_h^{n+\frac{1}{2}}, \nabla \cdot v_h) = (f(t^{n+\frac{1}{2}}), v_h) \qquad (5.5)\\ &(\nabla \cdot u_h^{n+1}, q_h) = 0 \qquad (5.6)\\ &\frac{1}{\Delta t}(B_h^{n+1} - B_h^n, \chi_h) + Re_m^{-1}(\nabla B_h^{n+\frac{1}{2}}, \nabla \chi_h) - b^*(\widetilde{B}_h^n, u_h^{n+\frac{1}{2}}, \chi_h)\\ &+b^{ast}(\widetilde{U}_h^n, B_h^{n+\frac{1}{2}}, \chi_h) + (\lambda_h^{n+\frac{1}{2}}, \nabla \cdot \chi_h) = (\nabla \times g(t^{n+\frac{1}{2}}), \chi_h) \qquad (5.7)\\ &(\nabla \cdot B_h^{n+1}, r_h) = 0 \qquad (5.8)\end{aligned}$$

Note that we could similarly derive the nonlinear scheme. All of the theoretical results follow as in the case of SV elements, but with the following exceptions: The velocity and magnetic fields will now only be weakly mass conservative, and the error estimate will now depend on the pressure error, although asymptotically the accuracy will be the same.

6 Numerical experiments

Here we run several numerical experiments to demonstrate the effectiveness of the scheme.

6.1 Experiment 1: Convergence rate verification

To verify our code, we compute convergence rates for a problem with known solution on a series of refined meshes and timesteps. We choose the test problem with solution

$$u = (1 + 0.01t) < \cos(y), \sin(x) >^T, \qquad B = (1 - 0.01t) < \sin(y), \cos(x) >^T$$

on the unit square with $Re = Re_m = 1$, endtime $T = 0.1$, and f and $\nabla \times g$ chosen accordingly. For our meshes, we use barycenter refinements of uniform meshes. Our coarsest mesh is shown in figure . The Scott-Vogelius elements (P_2, P_1^{disc}) are employed. From the convergence theory, we expect

$$\|u - u_h\|_{2,1} + \|B - B_h\|_{2,1} = O(\Delta t^2 + h^2).$$

The meshwidth and timestep are tied together so that when h is halved, so is Δt, and thus we expect to see second order convergence in this norm for both the velocity and magnetic field. The results of the simulations are given in Table 1, and we see precisely the expected behavior as the mesh and timestep decrease.

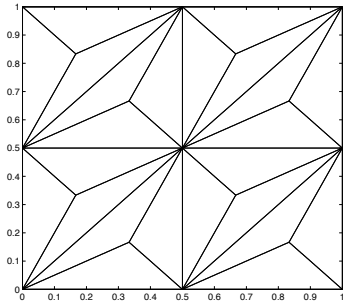

Figure 1: Shown above is the coarsest mesh used for computing convergence rates in numerical experiment 1. It is a barycenter refinement of a uniform mesh.

6.2 Experiment 2: Comparison of Scott-Vogelius and Taylor-Hood solutions

Because this is the first time the Scott-Vogelius element has been studied in this context, we compare its solutions with those obtained by using Taylor-Hood elements (and skew-

h	Δt	$dim(X_h)$	$dim(Q_h)$	Total dof	$\|u-u_h\|_{2,1}$	rate	$\|B-B_h\|_{2,1}$	rate
$\frac{1}{2}$	0.1	114	72	372	2.9482E-3	-	2.9409E-3	-
$\frac{1}{4}$	$\frac{0.1}{2}$	418	288	1,412	7.3699E-4	1.999	7.3576E-4	1.999
$\frac{1}{8}$	$\frac{0.1}{4}$	1,602	1,152	5,508	1.8427E-4	1.999	1.8403E-4	2.000
$\frac{1}{16}$	$\frac{0.1}{8}$	6,274	4,608	21,714	4.6063E-5	2.000	4.6010E-5	2.000
$\frac{1}{32}$	$\frac{0.1}{16}$	24,834	18,432	86,532	1.1515E-5	2.000	1.1503E-5	2.000

Table 1: The table above shows convergence of the computed mhd solution to the true solution, with the expected rates.

symmetrized nonlinear terms). We compute on the finest mesh that was used in experiment 1, a barycenter refinement of a 1/32 uniform triangulation of the unit square. We repeat the same problem as experiment 1, but set $T = 1$, $\Delta t = 0.01$, and compute for $Re = Re_m = 1$, $Re = Re_m = 10$, $Re = Re_m = 50$, and $Re = Re_m = 100$. Results are shown in Figures 2-5, and reveal fundamental differences between Scott-Vogelius and Taylor-Hood solutions.

The superiority of the Scott-Vogelius element solutions over the Taylor-Hood solutions is clear from Figures 2-5, especially as the Reynolds and magnetic Reynolds numbers increase. The difference that stands out the most is the oscillating error in the Taylor-Hood solutions, which puts the Taylor-Hood solution on a poor solution path from the first timestep - and progressively poorer as the Reynolds numbers increase, from which the solution never recovers optimal accuracy. The Scott-Vogelius solution, on the other hand, experiences very little initial oscillation, and its error appears nearly constant in time. For the $Re = Re_m = 100$ test, the error in the Taylor-Hood solutions is 2 orders of magnitude worse than for the Scott-Vogelius solution. In each of Figures, it can be seen that the divergence of the Scott-Vogelius solutions' velocity and magnetic field is near machine round-off, whereas for Taylor-Hood solutions the divergence is non-negligible.

6.3 Experiment 3: Orszag-Tang vortex

For our final experiment, we repeat a calculation done by J.-G Liu and W. Wang in [17] and by Friedel et. al. in [9]. We consider ideal 2D MHD, $Re = Re_m = \infty$, $\mathbf{f} = \nabla \times \mathbf{g} = \mathbf{0}$, $s = 1$, and compute on the 2π periodic box with initial condition

$$u_0 = < -\sin(y+2), \sin(x+1.4) >^T \qquad B_0 = < -\frac{1}{3}\sin(y+6.2), \frac{2}{3}\sin(2x+2.3) >^T$$

As discussed in [17], this configuration develops singularity-like structure known as current sheets where the current density grows exponentially in time, while the thickness shrinks at an exponential rate.

We compute with the linearized scheme (5.1)-(5.4) using (P_2, P_1^{disc}) Scott-Vogelius elements on a barycenter refinement of a uniform triangulation with $h = 1/64$ length sides. This provides 49,909 velocity nodes, which is about the number of nodes provided by a 223×223 finite difference grid. The total degrees of freedom was 345,092, and $\Delta t = 0.01$ timesteps were used up to $T = 2.7$.

Confirmation of the conservation properties of the scheme is shown in figure 6. Since this experiment is for ideal MHD, both energy and cross helicity should remain unchanged in time, and they do.

The plot of the current density at $t = 2.7$ is shown in figure 7. It agrees well with known results in [17, 9]. However, we note that a much coarser grid is used than in the experiments

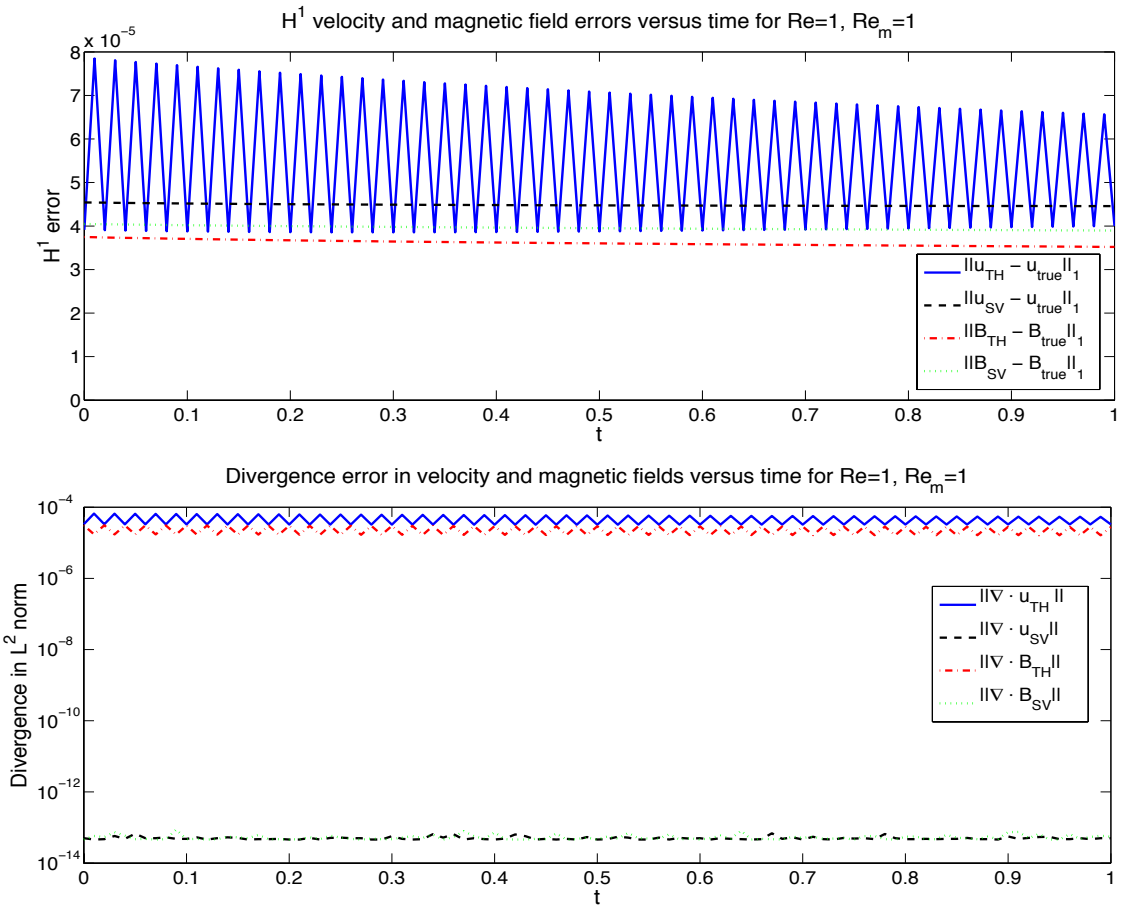

Figure 2: H^1 errors and error in divergence for the computed velocity and magnetic fields with $Re = Re_m = 1$.

we compare to: a grid of $1,024 \times 1,024$ was used in [17] and grids of up to $4,096 \times 4.096$ are used in [9].

7 Conclusion

A method was presented that allows to solve incompressible magnetohydrodynamic equations with strong enforcement of solenoidal constraints. This is crucial in many of the MHD applications, where (otherwise) different numerical techniques have to be adopted to enforce $\nabla \cdot u = 0$ and $\nabla \cdot B = 0$. In particular, our scheme should be of interest for those working on shock capturing in astrophysics. We prove the unconditional stability and optimal convergence of the scheme, and we demonstrate its physical fidelity by verifying that the energy, cross-helicity and magnetic helicity are conserved in the case of the ideal MHD. This leads to a better long time behaviour of the solutions obtained by our scheme. We also perform extensive computational tests, comparing our scheme to the standard approach that uses the Taylor-Hood finite elements. The difference is clear: the solutions obtained by using Taylor-Hood elements are oscillatory and the divergence of the velocity and magnetic field is nonzero, whereas the solutions obtained by our scheme do not have

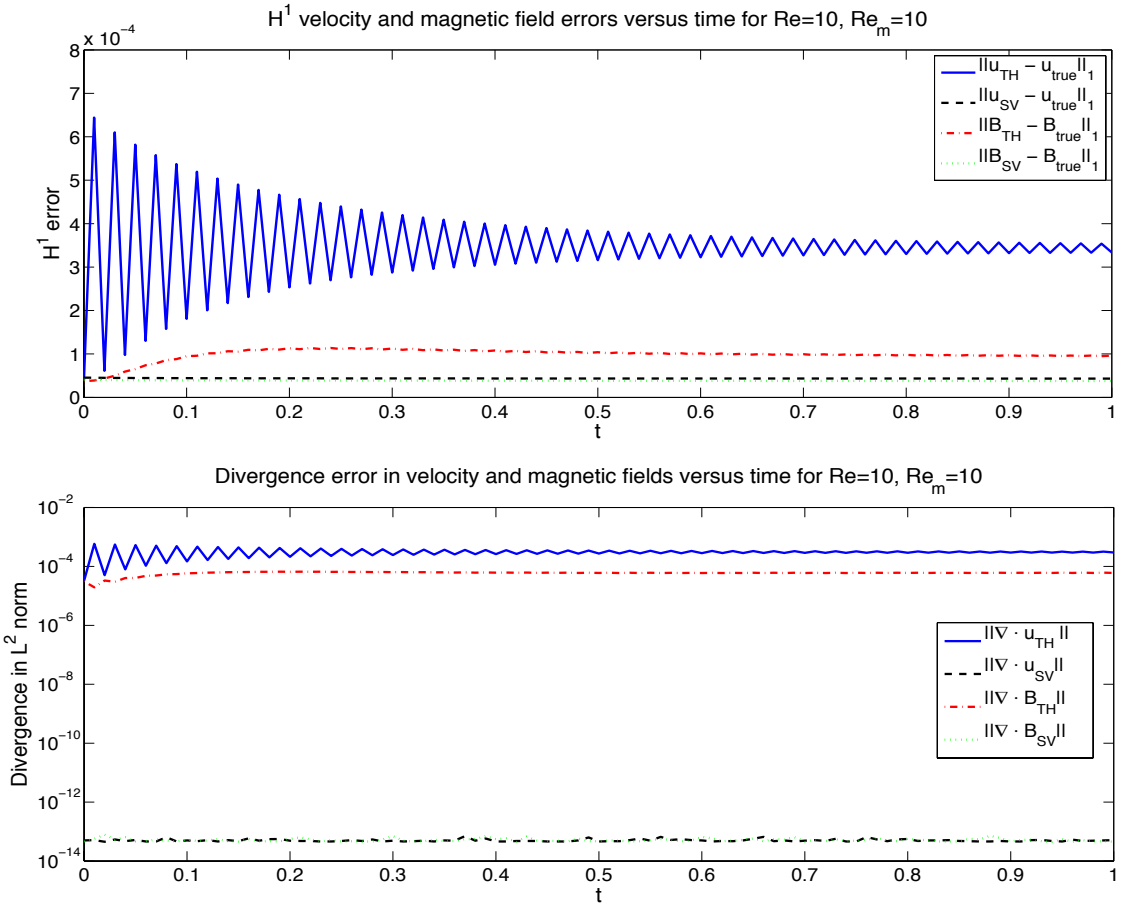

Figure 3: H^1 errors and error in divergence for the computed velocity and magnetic fields with $Re = Re_m = 10$.

these problems. Another important difference is that the nonphysical oscillations in the Taylor-Hood solutions increase as the Reynolds and magnetic Reynolds numbers increase, whereas the oscillations in the solutions obtained by our scheme are minimal and remain unchanged as Re and Re_m increase.This leads to a possibly very interesting investigation of employing the Scott-Vogelius finite elements in the problems with turbulence.

References

[1] A. Arakawa. Computational design for long-term numerical integration of the equations of fluid motion: Two dimensional incompressible flow, Part I. *J. Comput. Phys.*, 1:119–143, 1966.

[2] A. Arakawa and V. Lamb. A potential enstrophy and energy conserving scheme for the shallow water equations. *Monthly Weather Review*, 109:18–36, 1981.

[3] G. Baker. Galerkin approximations for the Navier-Stokes equations. Harvard University, August 1976.

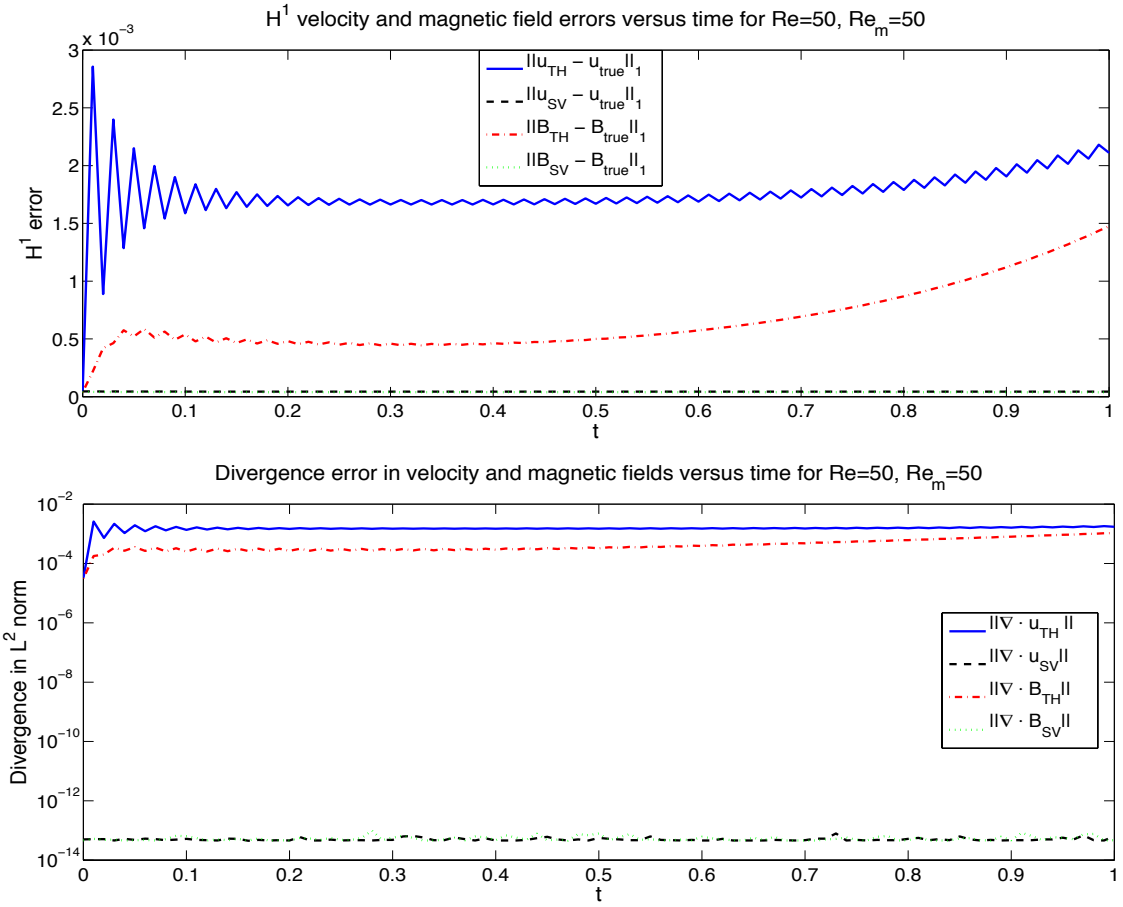

Figure 4: H^1 errors and error in divergence for the computed velocity and magnetic fields with $Re = Re_m = 50$.

[4] E. Burman and A. Linke. Stabilized finite element schemes for incompressible flow using scott-vogelius elements. *Applied Numerical Mathematics*, 58(11):1704–1719, 2008.

[5] M. Case, V. Ervin, A. Linke, and L. Rebholz. Improving mass conservation in FE approximations of the Navier Stokes equations using C^0 velocity fields: A connection between grad-div stabilization and Scott-Vogelius elements. *Submitted (available as tech report at http://www.wias-berlin.de/preprint/1510/wias_preprints_1510.pdf)*, 2010.

[6] M. Case, V. Ervin, A. Linke, L. Rebholz, and N. Wilson. Stable computing with an enhanced physics based scheme for the 3D Navier-Stokes equations. *International Journal of Numerical Analysis and Modeling*, to appear, 2010.

[7] P. Davidson. *An Introduction to Magnetohydrodynamics*. Cambridge, 2001.

[8] A. Dedner, F. Kemm, D. Kroner, C.-D. Munz, T. Schnitzer, and M. Wesenberg. Hyperbolic divergence cleaning for the mhd equations. *J. Comput. Phys.*, 175:645, 2002.

[9] H. Friedel, R. Grauer, and C. Marliani. Adaptive mesh refinement for singular current sheets in incompressible magnetohydrodynamic flows. *Journal of Computational Physics*, 134:190–198, 1997.

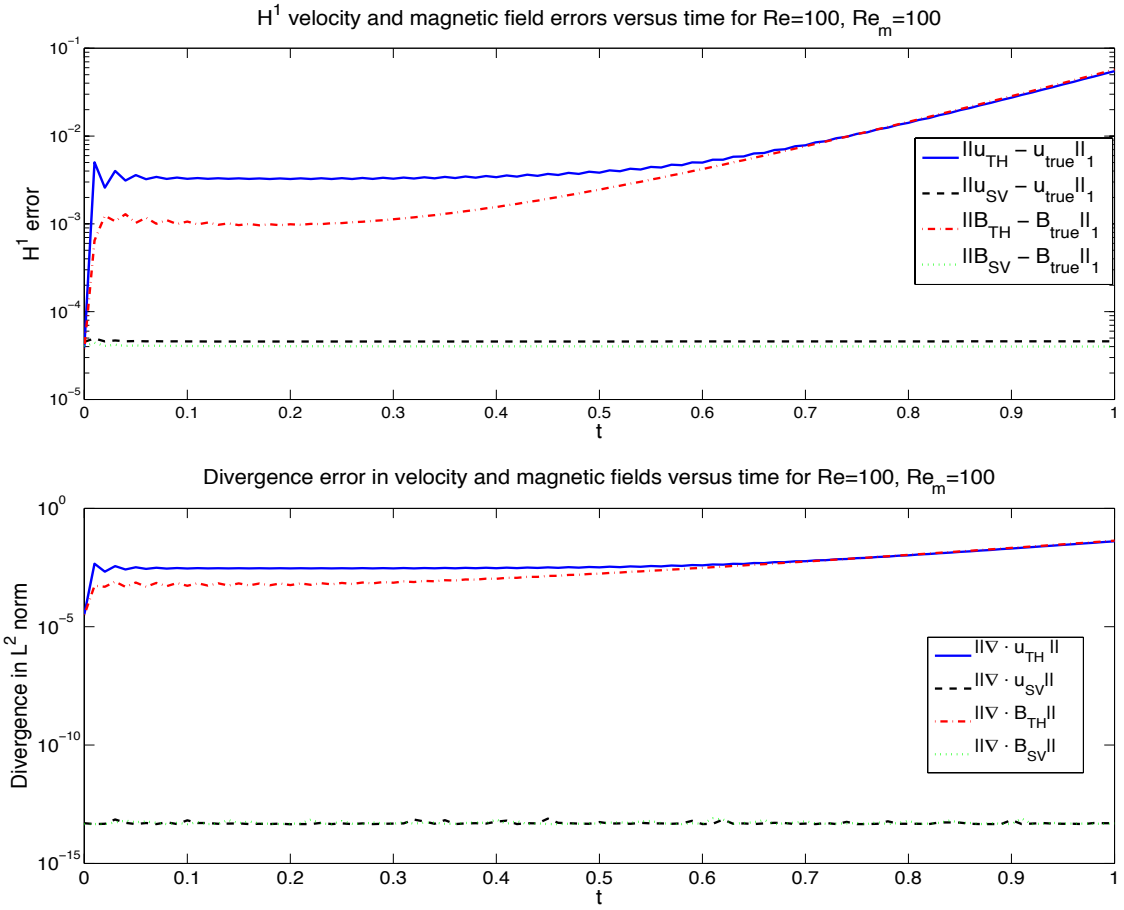

Figure 5: H^1 errors and error in divergence for the computed velocity and magnetic fields with $Re = Re_m = 100$.

[10] M. Gunzburger, O. Ladyzhenskaya, and J. Peterson. On the global unique solvability of intial-boundary value problems for the coupled modified Navier-Stokes and maxwell equations. *J. Math. Fluid Mech.*, 6:462–482, 2004.

[11] M. Gunzburger and C. Trenchea. Analysis and discretization of an optimal control problem for the time-periodic mhd equations. *J. Math Anal. Appl.*, 308(2):440–466, 2005.

[12] M. Gunzburger and C. Trenchea. Analysis of optimal control problem for three-dimensional coupled modified navier-stokes and maxwell equations. *J. Math Anal. Appl.*, 333:295–310, 2007.

[13] W. Layton. *An introduction to the numerical analysis of viscous incompressible flows.* SIAM, 2008.

[14] W. Layton, C. Manica, M. Neda, M.A. Olshanskii, and L. Rebholz. On the accuracy of the rotation form in simulations of the Navier-Stokes equations. *J. Comput. Phys.*, 228(5):3433–3447, 2009.

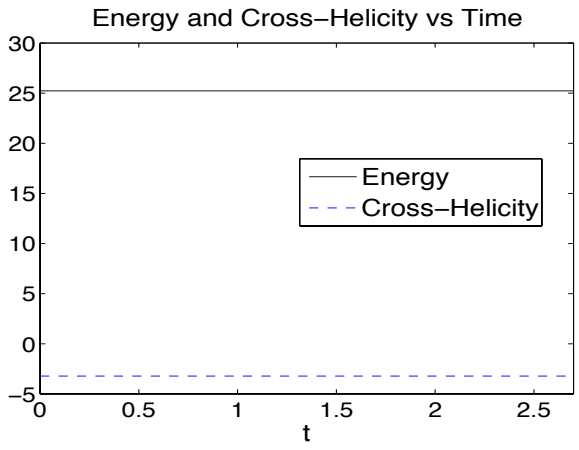

Figure 6: Energy and cross helicity versus time for numerical experiment 3; they are conserved.

[15] A. Linke. Collision in a cross-shaped domain — A steady 2d Navier-Stokes example demonstrating the importance of mass conservation in CFD. *Comp. Meth. Appl. Mech. Eng.*, 198(41–44):3278–3286, 2009.

[16] A. Linke, G. Matthies, and L. Tobiska. Non-nested multi-grid solvers for mixed divergence free scott-vogelius discretizations. *Computing*, 83(2-3):87–107, 2008.

[17] J. Liu and W. Wang. Energy and helicity preserving schemes for hydro and magnetohydro-dynamics flows with symmetry. *J. Comput. Phys.*, 200:8–33, 2004.

[18] J.-G. Liu and R. Pego. Stable discretization of magnetohydrodynamics in bounded domains. *Commun. Math. Sci.*, 8(1):234–251, 2010.

[19] I.M Navon. Implementation of a posteriori methods for enforcing conservation of potential enstrophy and mass in discretized shallow water equation models. *Monthly Weather Review*, 109:946–958, 1981.

[20] I.M. Navon. A Numerov-Galerkin technique applied to a finite element shallow water equations model with enforced conservation of integral invariants and selective lumping. *J. Comput. Phys.*, 52:313–339, 1983.

[21] L. Rebholz. An energy and helicity conserving finite element scheme for the Navier-Stokes equations. *SIAM Journal on Numerical Analysis*, 45(4):1622–1638, 2007.

[22] R. Temam. *Navier-Stokes equations : theory and numerical analysis*. Elsevier North-Holland, 1979.

[23] M.S. Yalim, D.V. Abeele, and A. Lani. Simulation of field-aligned ideal mhd flows around perfectly conducting cylinders using an artificial compressibility approach. *Hyperbolic Problems: Theory, Numerics, Applications*, 4:1085–1092, 2008.

[24] S. Zhang. A new family of stable mixed finite elements for the 3d stokes equations. *Mathematics of Computation*, 74:543–554, 2005.

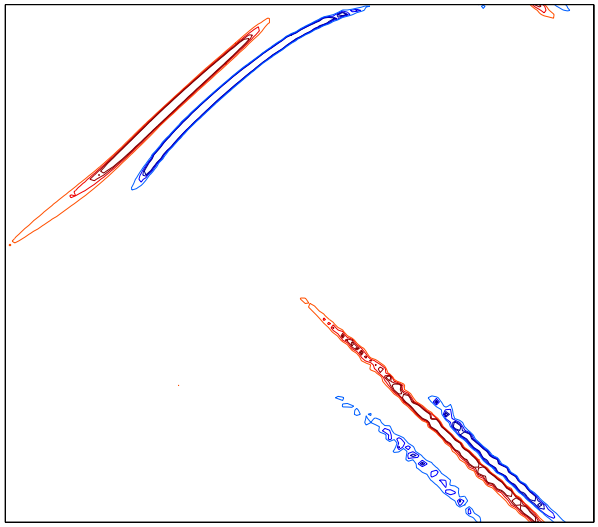

Figure 7: Current density $|\nabla \times B|$ at $t = 2.7$.